Oxidative degradation of sulfamethoxazole from secondary treated effluent by ferrate(VI): kinetics, by-products, degradation pathway and toxicity assessment

Behjat Jebalbarezi[1,2] · Reza Dehghanzadeh[1] · Samira Sheikhi[2] · Najmeh Shahmahdi[1] · Hassan Aslani[3] ·
Ammar Maryamabadi[4]

Abstract

Sulfamethoxazole (SMX) is a typical antibiotic in the world, which is frequently detected in the aquatic environment. The current study was aimed to investigate the SMX degradation in secondary treated wastewater using potassium Ferrate [Fe(VI)]. The effects of various experimental conditions, EDTA and phosphate as chelating agents, and toxicity assessment were also considered. Secondary treated effluent was spiked with predefined SMX concentrations, and after desired reaction time with Fe(VI), residual SMX was measured using HPLC. Results indicated that SMX degradation by Fe(VI) was favored under acidic condition, where 90% of SMX degradation was achieved after 120 min. Fe(VI) and SMX reaction obeyed first-order kinetic; meantime, the SMX degradation rate under pH 3 was 7.6 times higher than pH 7. The presence of phosphate (Na_2HPO_4) and EDTA declined SMX degradation, while Fe (III) effect was contradictory. In addition to promising demolition, 10% TOC removal was achieved. Eighteen major intermediates were identified using LC-MS/MS and the degradation pathways were suggested. Transformation products (TPs) were formed due to hydroxylation, bond cleavage, transformation after bond cleavage, and oxidation reactions. The ECOSAR analysis showed that some of the SMX oxidation products were toxic to aquatic organisms (fish, daphnia and green algae).

Keywords Sulfamethoxazole · Fe(VI) process · Degradation products · Wastewater · ECOSAR

Introduction

The presence of significant amounts of antibiotic residues in aquatic environments has recently become a main concern in the world [1–3]. Antibiotics, as an essential part of pharmaceuticals, are used to control infections and improve the health of humans and animals in medicine and dentistry [4, 5]. Some parts of these antibiotics are excreted without absorption in the human or animal body [6, 7]. On the other hand, it is reported that in some developing countries, pharmaceutical substances are discharged into natural environments without any restriction. Although their entry into the aqueous medium is not very high, their continuous entry, due to the cumulative effects, there may be a severe threat to the humans, ecosystem and microorganisms [8].

Sulfonamides are a group of antibiotics that have recently received special attention due to the high rate of excretion and stability in the environment. Sulfamethoxazole (SMX), an antibacterial sulfonamide, is known as an important environmental antibiotic due to its properties

Highlights
- The conditions of SMX degradation process were investigated.
- Fe(VI) oxidation was effective for SMX removal.
- Some of the toxic products were generated during SMX oxidation.
- ECOSAR analysis was performed to assess the SMX environmental risks.

✉ Hassan Aslani
haslani@tbzmed.ac.ir

1 Student research committee, Tabriz University of Medical Sciences, Tabriz, Iran

2 Department of Environmental Health Engineering, Tabriz University of Medical Sciences, Tabriz, Iran

3 Health and Environment Research Center, Tabriz University of Medical Sciences, Tabriz, Iran

4 R&D Department, Shakheh Zeytoon Lian Co., Bushehr, Iran

such as abundance in aqueous media, stability and resistance, high biological storage, toxicity and bioavailability [9, 10]. Recent researches have represented that antibiotics can change the genomes of microbial communities in aquatic ecosystems, helping to create antibiotic-resistant bacteria and genes [11]. The conventional treatment processes cannot wholly eradicate resistant organics such as antibiotics [12, 13]; consequently, the frequent presence of SMX in aquatic environments has been perceived [14]. Therefore, in order to reach the standards of drinking water, it is necessary to apply more efficient and appropriate treatment processes in a way that removes drug substances and similar contaminants [15, 16]. The findings of previous studies have demonstrated that although techniques such as electrocoagulation, adsorption and membrane processes can be considered to eliminate medicine compounds, but the use of these techniques due to low efficiency, high investment costs, management and maintenance problems is less likely [1, 17].

Iron-based oxidation technologies have recently received more attention because iron is one of the most abundant elements and is environmentally friendly [18]. In addition, some of the iron-containing substances are easily separable and recyclable after the treatment process due to their magnetic nature [19]. In some developed countries, ferrate (Fe(VI)) is used for disinfection, oxidation or coagulation purposes [20]. Ferrate has a strong oxidation capacity, which in acidic and alkaline conditions varies from 2.2 to 0.7 V, respectively [21, 22]. In general, ferrate is a multi-function agent applied for the oxidation of synthetic organic/inorganic contaminants, elimination of humic substances, coagulation, and disinfection of water, wastewater, and sludge samples [23, 24]. Ferric oxide is a strong coagulant that can be produced from the Fe(VI) self-decomposition and eliminate various metals, non-metals and some organic matter. Fe(VI) is able to inactivate a wide range of microorganisms in low concentrations over short periods of time [25]. Several studies have evaluated the efficiency of potassium ferrate in removing contaminants from water and wastewater [26–29]. Fe(VI) is a potent oxidant with fewer environmental side effects than many other chemical oxidants, so many efforts have been made to eliminate various antibiotics and the resulting metabolites by using it [30–33]. Some similar studies have examined the removal of SMX with Fe(VI) [34–36]. However, most of them focused on reaction kinetics. Also, in these studies, the selective matrix was pure water and therefore the role of wastewater constituents such as phosphate, iron, and EDTA was not fully considered. In the present study, in addition to investigating the role of these compounds, the toxicity of SMX and its degradation byproducts has been evaluated. In this paper, we systematically investigated the removal of SMX from secondary treated effluent by Fe(VI). The targets of this work were (a) investigating the effects of the operational parameters

(pH, contact time, Fe(VI) and SMX doses, effect of EDTA, phosphate and iron ions) on SMX degradation, (b) determination of reaction kinetics, (c) propose the degradation pathways of SMX, (d) determination of SMX byproducts during the process and (e) toxicity assessment of SMX and its byproducts on three typical aquatic species (fish, daphnia and green algae).

Materials and methods

Materials

SMX (>98.0%) was prepared from Iran Daru Co., Ltd. (Tehran, Iran). Potassium ferrate (K_2FeO_4,>98.0%) in solid form was purchased from BOC Sciences (New York, USA). Other chemicals including methanol (CH_4O, chromatographic grade), acetonitrile (CH_3CN), dichloromethane (CH_2Cl_2), sodium thiosulfate ($Na_2S_2O_3$), citric acid ($C_6H_8O_7$), sodium hydroxide (NaOH), hydrochloric acid (HCl), methyl tert-butyl ether ($C_5H_{12}O$), disodium hydrogen phosphate (Na_2HPO_4), $FeCl_3.6H_2O$ and EDTA (>99.0%) were purchased from Merck Co. (Darmstadt, Germany). All the mentioned chemicals were in the analytical grade.

Experimental procedures

Sample preparation and experiments

Details related to secondary treated effluent (STE) used in the study are listed in Table 1. The samples were collected from Tabriz municipal wastewater treatment plant and transferred to the university laboratory in polyethylene containers and kept in the refrigerator until the experiments were performed. A 0.22 μm nylon filter was used to filter the samples. Then, SMX in desired concentration was spiked to the samples. The effects of Fe(VI) dose (1-10 mg/L as Fe), pH

Table 1 STE physicochemical properties

N	Parameter	Mean value (SD)	Unit
1	TSS	$300 \pm (14)$	mg L^{-1}
2	VSS	$10 \pm (2)$	mg L^{-1}
3	COD	$38 \pm (12)$	mg L^{-1}
4	TOC	$19 \pm (3)$	mg L^{-1}
5	N-NO$_3^-$	$7.8 \pm (5)$	mg L^{-1}
6	N-NO$_2^-$	$0.06 \pm (0.01)$	mg L^{-1}
7	SO$_4^-$	$91.18 \pm (13)$	mg L^{-1}
8	PO$_4^-$	$3.83 \pm (0.6)$	mg L^{-1}
9	Cl$^-$	$103.96 \pm (20)$	mg L^{-1}
10	Alkalinity	$124 \pm (18)$	mg L^{-1} as CaCO3
11	pH	$7.5 \pm (0.3)$	–

(3-9), SMX initial concentration (200 and 1000 μg/L) and reaction time (5-60 min) on SMX degradation were evaluated. Afterwards, the process efficiency was determined by changing each variable at a time. All the experiments were conducted in duplicate at 25 ± 2 °C.

The experiments were performed in reactors which were completely mixed using a standard six paddle Jar test machine (180 rpm). In the first step, 1000 ml of SMX spike effluent was poured into the reactor and subsequently, Fe(VI) was added to the solution at the desired concentration. Then, pH was adjusted with 1 M NaOH or HCl. At defined time intervals, 15 ml of the sample was taken and quenched by the addition of 25 μl of 3% $Na_2S_2O_3$. After assessing the optimum conditions at the end of the experiments, total organic carbon (TOC) and chemical oxygen demand (COD) were measured based on the standard methods for water and wastewater examination [37]. For a better understanding of Fe(VI) performance in SMX mineralization and reducing the detrimental effects of wastewater constituents, the COD and TOC experiments were conducted in double distilled water under optimum conditions. Moreover, for assessing spontaneous SMX degradation in different pHs, the control experiments were performed in parallel, without the addition of Fe(VI).

Kinetics study

The kinetic investigation was accomplished under optimal conditions for a deep understanding of SMX degradation using Fe(VI). The kinetics of the reactions provides useful information about the reaction speed and the mechanism of converting reactive substances. The mathematical relation between reaction rate and reactant concentration is called the speed equation [38]. Various kinetic equations (zero-order, first-order and second-order) were used to describe the Fe(VI) oxidation kinetics.

Determine the effect of EDTA, phosphate and iron

To identify the conduct of the Fe(VI) in the degradation of SMX, the effect of EDTA, as a Fe(VI) complexing agent, was examined. In addition, the effects of phosphate (Na_2HPO_4) and iron ($FeCl_3$) ions on SMX degradation were evaluated. The oxidation of SMX using Fe(VI) under optimal conditions (were determined in the previous stages of the study), was evaluated at different initial concentrations of EDTA (0, 2, 4 mM), $FeCl_3$ (0, 0.048, 0.096, 0.145, 0.2 μM) and Na_2HPO_4 (0, 0.2, 0.5, 1.2 μM). It should be noted that, for a correct understanding of these compounds on Fe(VI) performance for SMX degradation and avoiding secondary treated effluent matrix interference in result interpretation, all experiments in this part were conducted in pure water media.

Analytical methods

SMX concentration in samples was measured using high-performance liquid chromatography (HPLC, Agilent, Germany) using a Restek SB-C18 column (4.6×250 mm, 5 μm) equipped with an UV detector at 270 nm. The mobile phase was HPLC grade ultra-pure water (60%) and acetonitrile (40%) with a flow rate of 1 mL/min. Samples with a volume of 20 μl were injected into the column for separation at 32 °C.

Identification of intermediate products resulting from SMX decomposition during the oxidation process was performed using an LC-MS/MS (Waters Corporation, USA) connected to an electrospray source and a positive ionization separator. SMX and intermediate products were separated by a C18 column (Penomenex Gemini) (100 mm×2 mm ID×5 μm). The mobile phase is composed of phase A (water/acetonitrile 90:10 and formic acid 0.1%) and phase B (water/acetonitrile 10:90 and formic acid 0.1%) with a flow rate of 0.4 mL/min. Positive ESI source specifications: capillary voltage 4 kV, extractor 1 V, evaporator temperature 300 °C, and source temperature 110 °C. The flow rate of cone gas and desolvation gas were 50 and 1000 L/h, respectively. The data were scanned at 50-550 m/z. This part of the experiments was performed in pure water to prevent the detrimental effect of complex effluent matrices. TOC and COD were analyzed according to the 5310 B and 5220 D standard methods for water and wastewater treatment, respectively. The pH was measured by EDT pH meter (London, UK).

Toxicity estimation

The ecological structure activity relationship (ECOSAR) computer program (version 2.0) was used to evaluate the acute and chronic toxicity of SMX and its TPs. This simulation program is widely developed and approved by USEPA, OECD and EU. Therefore, acute toxicity was shown with LC_{50} values for fish and daphnia as well as EC_{50} for green algae. Also, the value of chronic toxicity (ChV) was estimated for each product.

Results and discussion

Effect of the solution pH

The Fe(VI) oxidation power is dependent on the pH conditions. The experiments were carried out with an initial SMX concentration of 1000 μg/L and pH values of 3, 5, 7, and 9. The SMX removal variations at different pHs are shown in Fig. 1A. According to the results, it can be seen that by increasing pH, while other variables kept constant, antibiotic removal efficiency decreased, and the highest removal
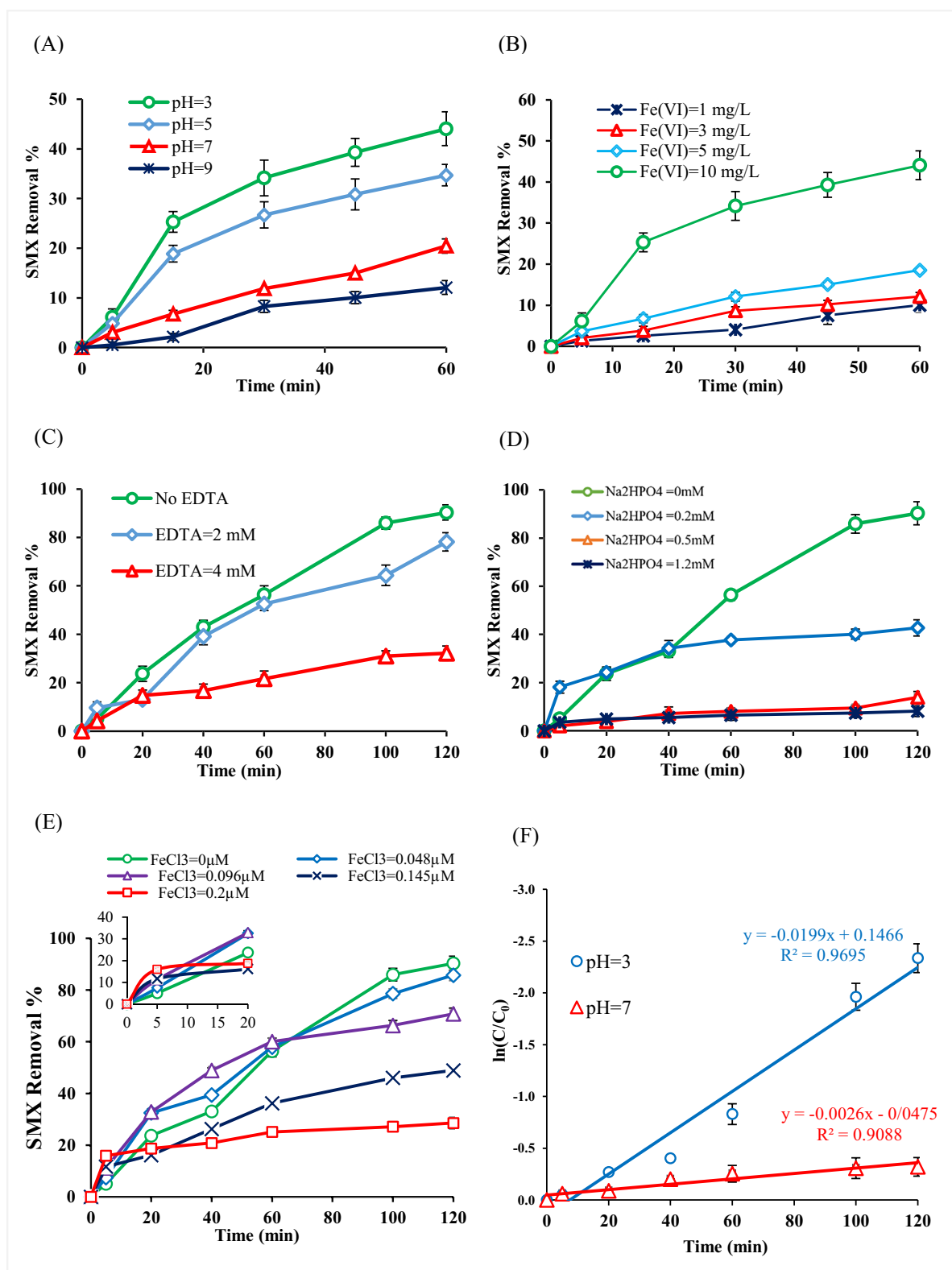
Fig. 1 Effect of (**A**) pH, (**B**) oxidant doses, (**C**) EDTA, (**D**) Na$_2$HPO$_4$ and (**E**) FeCl$_3$ on the removal of SMX by Fe(VI). Typical experimental conditions: [SMX]$_0$ = 1000 µg /L, [Fe(VI)]$_0$ = 10 mg/L at laboratory temperature. (**F**) First-order reaction kinetics of SMX removal.

Experimental conditions: [SMX]$_0$ = 1000 µg/L, Fe(VI) = 10 mg/L and initial pH = 3 and 7. (**G**) TOC and COD removal and (**H**) Evolution of sulfate and nitrate ions as a function of time at the optimal conditions mentioned above
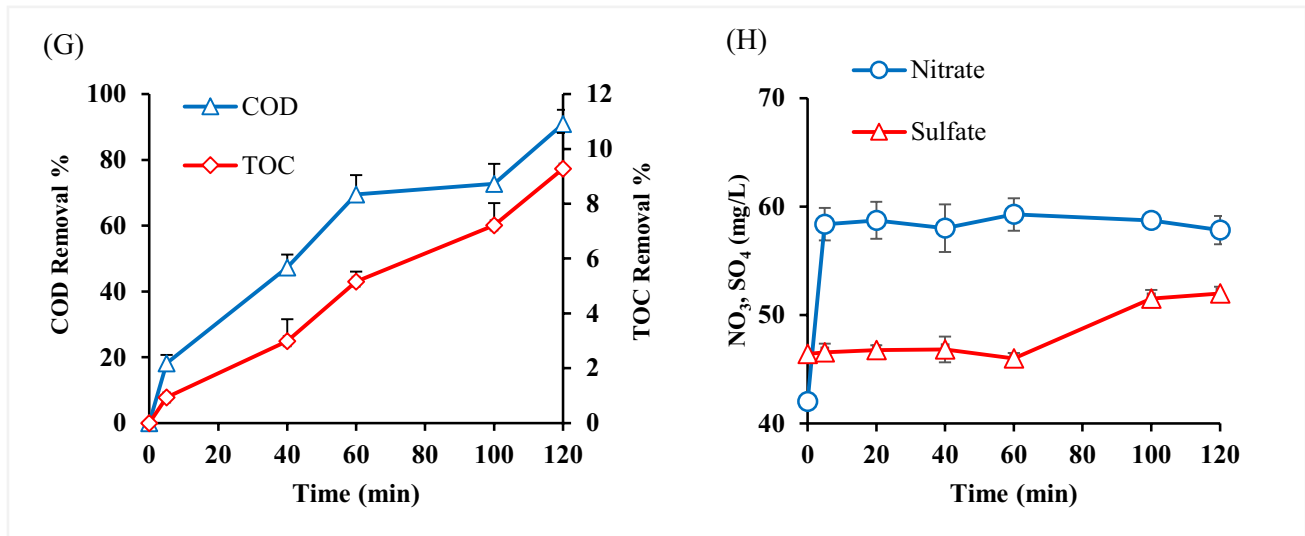
Fig. 1 (continued)

efficiency of 44.05% was achieved at pH = 3. SMX oxidation was significantly weakened in alkaline conditions. The pH effect can be described using considering the produced iron species and SMX equilibrium in different pHs. According to Eqs. (1)-(3), Fe(VI) in terms of solution pH forms different types including $H_3FeO_4^+$, H_2FeO_4, $HFeO_4^-$ and FeO_4^{2-} [39, 40]. At low pH (3 and less) conditions, the main species of Fe(VI) in aqueous solution are $H_3FeO_4^+$ and H_2FeO_4, considering the lower pKa of these species and their superior oxidation potential, higher removal efficiency is expected compared to the alkaline pH [24, 41]. It has been reported that the dominant species at acidic and alkaline pH were $HFeO_4^+$ and FeO_4^{-2}, respectively [42].

$$H_3FeO_4^+ \rightarrow H^+ + H_2FeO_4 \qquad (pK_a = 1.6) \tag{1}$$

$$H_2FeO_4 \rightarrow H^+ + HFeO_4^- \qquad (pK_a = 3.5) \tag{2}$$

$$HFeO_4^- \rightarrow H^+ + FeO_4^{2-} \qquad (pK_a = 7.3) \tag{3}$$

The sampling was performed in specified time intervals for 60 min to consider the impact of reaction time on SMX degradation by Fe(VI). It is obvious from Fig. 1A that at the first 15 min of the reaction time, in pH values of 3 and 5, there is a significant increase in SMX removal, followed by a gradual trend in the next 30 min, that is consistent with similar studies [34, 43]. On the other hand, under neutral and alkaline pH conditions, after 30 min, no considerable change in SMX concentration was observed with increasing contact time. Investigating the effect of reaction time on the SMX removal process showed that with increasing time, Fe(VI)

efficiency increased, and the highest removal efficiency of nearly 45% was recorded after 60 min, which is consistent with Jiang et al. [33]. In a similar study, Deng et al. (2019), by examining the removal of ciprofloxacin antibiotics using Fe(VI), reported that the removal of ciprofloxacin occurs mainly in the first 2 min and the removal is gradual in the next 12 min [31]. This reaction trend can be attributed to the less active iron species availability resulted from Fe(VI) decomposition in longer reaction times [34].

Effect of Fe(VI) dosage and SMX concentration

The effect of different Fe(VI) doses (1, 3, 5, and 10 mg/L as Fe) was investigated on 200 and 1000 µg/L SMX at optimal pH 3. Figure 1B shows the average SMX removal during certain sampling times. It can be seen that in Fe(VI) doses between 1 and 5 mg/L, the removal efficiency was less than 20% after 60 min reaction time. In other words, increasing Fe(VI) dosage from 1 to 5 mg/L did not show significant improvement in the removal of SMX. However, when Fe(VI) dosage increased to 10 mg/L, a meaningful change occurred in SMX removal, and the maximum removal efficiency of 44% was attained after 60 min. It should be considered that when Fe(VI) dose was doubled, i.e., extended from 5 to 10 mg/L, the removal efficiency increased about 2.5 times in all sampling times. One reason may be that the ratio of Fe(VI) self-decomposition is lower in higher concentrations. Therefore, it can affect the removal of SMX [31]. In addition, the higher efficiency of the process at higher doses of Fe(VI) may be due to the faster production of Fe oxidizing species, resulting from an increase in active ions [44]. The findings in this area are consistent with the results presented in the previous literature [31].

The effect of initial antibiotic concentration (200 and 1000 μg/L) on removal efficiency was also considered. The results indicated that in low concentrations of Fe(VI) (1-3 mg/ L), removal efficiency in the reactor containing 200 μg/L of SMX was higher than 1000 μg/L of SMX; while this procedure was reversed in high Fe(VI) dosage (Fig. S1). As more oxidizing species are available at higher Fe(VI) concentrations, the possible collision of SMX and oxidizing species is expected to increase, leading to increased process efficiency. The finding of this part of the study is well compatible with the previous studies [45]. Based on the results mentioned above, the optimum conditions of all the variables are as follows: pH = 3, initial concentration of SMX = 1000 μg/L, and Fe(VI) concentration = 10 mg/L. Afterward, all experiments were performed under optimum conditions and reaction time was extended until 120 min.

Effect of EDTA

EDTA, as a chelating agent, and its effect on SMX destruction by Fe(VI) was investigated. It has been reported that EDTA is an effective chelating agent in Fe-based processes [46]. Since EDTA can create various heavy metals complexes in water and wastewater treatment processes, it can be used for the recovery of these metals [47]. As shown in Fig. 1C, in the absence of this chelating agent, SMX degradation by Fe(VI) reached 90.32% after 120 min. However, the amount of SMX degradation in the attendance of 2 (Fe:EDTA = 0.09) and 4 (Fe:EDTA = 0.045) mM EDTA declined to 77.54% and 31.94%, respectively. According to the findings of this study, it is obvious that EDTA could significantly reduce SMX decomposition and tackles the oxidation effects of Fe(VI). It has been proven that the Fe(VI) decomposition rate in the presence of EDTA is much lower compared to the absence of EDTA in the solution. Consequently, it can be said that EDTA is one of the main interfering factors at Fe(VI) oxidation [48–50].

Effect of phosphate ion

Phosphate is more commonly found in industrial and urban wastewaters and surface waters such as rivers, receiving either raw wastewater or agricultural runoff [27]. It has been reported that phosphate ions can form internal complexes with Fe (III) oxide/hydroxide, thus accelerating the self-decomposition of Fe(VI) and interacting rapidly with organic pollutants [31, 39, 51]. The effects of different phosphate concentrations (0.2-1.2 mM of Na_2HPO_4) on SMX degradation were examined and the results are shown in Fig. 1D. At the first 5 min, the lowest phosphate used (0.2 Mm) accelerated SMX degradation. However, when the reaction time proceeded, the removal efficiency significantly declined compared to the condition without phosphate. It is evident that after 120 min, removal efficiency in the presence of 0.2 mM Na_2HPO_4 decreased to 48%. On the other hand, the higher phosphate concentrations (0.5 and 1.2 mM Na_2HPO_4) showed antagonistic effects on SMX degradation. Therefore, the removal efficiency decreased to 13 and 8%, respectively. Complexation of active Fe species, such as Fe(V) and Fe(IV), with phosphate, possibly can explain this variation as stated in previous studies [52]. Chemically, the phosphate anion as the Lewis base can donate its electron pair from oxygen atoms to transition metals orbital and produce complexes. In reaction with Fe(VI), phosphate anions may attack the iron center of Fe(VI) as a nucleophile and lead to the reconstitution of the coordination pair from four to six coordinates [53]. The complexity with ligands can change redox potential [54]. The combination of Fe(VI) with phosphate ligand may decrease its potential yield and have a negative effect on the Fe(VI) reaction with organic compounds, SMX in this study. Coordination with phosphate ligands results in the expansion of the coordinated Fe(V) structure from tetrahedral to octahedron geometry that may prevent the combination of Fe(VI) with the goal compounds and affect the electron transfer procedure [55]. Hence, this complexation may reduce the amount of Fe(VI) besides its self-decomposition rate [52].

Effect of iron ion

The results of the effect of iron ion ($FeCl_3$) on SMX removal are shown in Fig. 1E. The present study was conducted at optimum condition and iron concentrations of 0 to 0.2 μM, as $FeCl_3$, under extended reaction time. As represented in Fig. 1E, the iron effect on SMX removal by Fe(VI) is not constant during the process. On the one hand, lower iron concentrations (0.048 and 0.096 μM) could mildly improve process performance in earlier reaction time, i.e., until 60 min. However, no substantial change was observed by the end of the process. It can be noted that iron in this range did not dramatically affect the process. On the other hand, higher iron concentrations (0.145 and 0.2 μM) influenced the process reversely, and a clear decline in process efficiency can be noticed in the whole sampling times. It is evident in Fig. 1E that when 0.2 μM iron was present in the solution, removal efficiency almost decreased three times in comparison to the control sample. Our findings in this regard conflicted with those reported by Zhao et al. (2018). They reported that both Fe(III) and Fe(II) revealed a catalytic effect on diclofenac degradation by Fe(VI) [52].
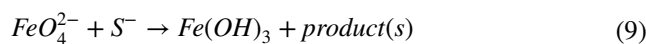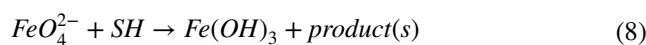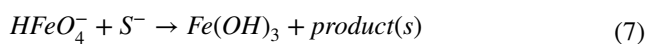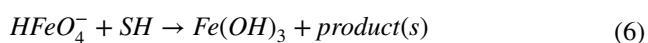
Kinetic study

In all oxidation processes, the kinetic study of the reaction is performed to better understand how the contaminant reacts with oxidation agents. Kinetic studies significantly contribute

to process modelling and implementation at the application scale. The above assumptions and the degree of reaction can be examined by drawing a semi-logarithmic graph of the concentration of SMX over time. The SMX degradation was studied under optimum Fe(VI) dosage and prolonged reaction time to determine the speed of SMX degradation. The optimum pH of experiments was 3, which is not appropriate for reactions that occur in natural environments (wastewater treatment plants, for instance). To simulate the actual situation, kinetic experiments were performed under two different pH (3 and 7) at laboratory temperature. Considering the zero, first, and second-order kinetics, SMX degradation was best fitted to the first-order model, shown in Fig. 1F. The first-order reaction rate (k) for pH 3 and 7 are 1.9×10^{-2} and 2×10^{-3} min^{-1}, respectively and the amount of R^2 for pH 3 and 7 are 0.9695 and 0.9088, respectively. By comparing the degradation rate between the two pH conditions, it can be inferred that the SMX degradation rate under pH 3 is 7.6 times faster than pH 7. It should be noted that in pH 3, almost 90% of SMX was degraded after 120 min, and the R^2 value was nearly 0.97, while in pH 7 only 27% degradation was observed, and the R^2 value was 0.9. Therefore, it can be concluded that the degradation of SMX by the Fe(VI) process in acidic conditions is more favorable. The change of k value with the pH change can be explained by the balance of mono protonated ferrate ($HFeO_4^-$) and SMX, as shown in Eqs. 4 and 5 [56, 57].

$$HFeO_4^- \leftrightarrow H^+ + FeO_4^{2-} \qquad \left(pK_{a.HFeO_4^{2-}} = 7.23 \right) \qquad (4)$$

$$SH\ (SMX) \rightarrow H^+ + S^- \qquad \left(pK_{a.SH} = 5.5 \right) \qquad (5)$$

According to Sharma et al. (2001), as revealed in Eqs. 6 to 9, in the pH range under study, two forms of mono-protonated Fe(VI) can react with two SMX forms.

$$HFeO_4^- + SH \rightarrow Fe(OH)_3 + product(s) \qquad (6)$$

$$HFeO_4^- + S^- \rightarrow Fe(OH)_3 + product(s) \qquad (7)$$

$$FeO_4^{2-} + SH \rightarrow Fe(OH)_3 + product(s) \qquad (8)$$

$$FeO_4^{2-} + S^- \rightarrow Fe(OH)_3 + product(s) \qquad (9)$$

Ferrate mono-protonated species, $HFeO_4^-$, in the pH range under study as mentioned in the literature, are the most reactive species [39, 58–60]. Higher Fe(VI) self-decomposition as well as higher $HFeO_4^-$ species in the acidic pH range can explain a higher reaction rate in pH 3 compared to pH 7. Also, the larger spin density of $HFeO_4^-$ species in oxo ligands than FeO_4^{2-} and partial radical character of Fe(V) can increase $HFeO_4^-$ reactivity with SMX. A comparison of the degradation rate of different antibiotics by Fe(VI) with the present study is presented in Table 2. Because various experimental conditions (e.g., initial pH, Fe(VI) dosage and antibiotic concentration) cannot be adjusted between different studies, definitive conclusions are not possible. However, according to Table 2 and the experimental conditions, the degradation rate in the present study is consistent with the results presented in the previous literature.

COD and TOC removal under optimal experimental conditions

The effect of Fe(VI) on the COD and TOC removal at optimum conditions is shown in Fig. 1G. It is evident from this Figure that COD removal is many times more than TOC removal. In other words, the concentration of COD was significantly reduced by Fe(VI). It is also clear that removal efficiency increases over reaction time, and after 120 min, 90% removal is obtained. As shown in Fig. 1G, it can be seen that the removal efficiency increased sharply to 40 min, while from this point on, it continued with a gentle slope. It has been reported that potassium ferrate was able to decrease COD to 52% after 30 min contact time [61]. The highest TOC removal using Fe(VI) was about 10%, obtained after 120 min of contact time. Incomplete mineralization of SMX shows some of its TPs were not easily oxidized by Fe(VI). TOC analysis and mineralization of organic matter can help

Table 2 Comparison of Fe (VI) oxidative potential for different antibiotics

Compound	K (min^{-1})	Initial concentration (mM)		pH	Time (min)	Reference
		antibiotic	Fe(IV)			
sulfonamide	1.9×10^{-1}	0.06	1.01	3	60	[85]
chloramphenicol	9.9×10^{-3}	0.003	0.25	6	60	[86]
sulfadiazine	1.1×10^{-2}	0.06	0.8	7	60	[73]
diclofenac	2.2×10^{-2} [a]	0.08 [b]	24 [b]	7	120	[87]
diclofenac	4.6×10^{-3} [a]	0.03	0.45	7	120	[87]
sulfamethoxazole	1.8×10^{-1}	0.06	1.01	3	60	[85]
sulfamethoxazole	1.9×10^{-2}	0.004	0.18	3	120	This Study

a: k units are S^{-1}, b: units are μM

to identify the pathway of pollutants degradation [62]. Following the oxidation process, large amounts of SMX are converted to intermediates that may be more toxic compared to the parent compound [63]. Therefore, to better evaluate the effects of oxidation processes, it is better to identify transformation products.

Inorganic ions evolution during the process

Mineralization of organic materials containing heteroatoms can be associated with the inorganic ions release, including nitrate, nitrite, and sulfate. The formation of organic ions was considered as an indicator of SMX mineralization. SMX molecule bond cleavage will release the S as sulfate ion (SO_4^{2-}), and the N atoms are transferred to nitrate, nitrite, and ammonia. Figure 1H indicates the nitrate and sulfate variation during the oxidation process [64]. It is noteworthy that in the present study, no nitrite or ammonia was detected. It is clear from Fig. 1H that nitrate release occurred in the first 5 min of the experiment, when Fe(VI) self-decomposition products (Fe(V) and Fe(IV)) with strong oxidation potential may attack SMX bonds. From this point until the end of the process, the nitrate concentration was almost constant, which is related to the rapid decomposition of and Fe(VI) reactivity. In the case of sulfate, it is evident that no increase was observed until 60 min, which could be attributed to either sulfate reaction with iron species, particularly Fe(III) or sulfate adsorption by metal oxide surfaces [64]. From this point on, sulfate release can be clearly traced, indicating SMX mineralization.

Degradation pathway and products

The LC-MS/MS technique was used to identify the SMX degradation intermediates using the Fe(VI) process. This experiment was conducted at pH = 3, SMX initial concentration = 2 mg/L, Fe(VI) dosage = 10 mg/L and reaction time = 180 min. The SMX degradation pathways during Fe(VI) oxidation are shown in Fig. 2. Also, all of the detected products with molecular formula and their mass charge ratio (m/z) are listed in Table 3. As shown in Fig. 2, nine possible degradation pathways were identified.

The SMX has a molecular ion peak of m/z 253 ([M+H]$^+$) [65]. The O-N bond of the isoxazole ring was broken down through isomerization to produce TP253 from SMX [66]. TP283a and TP283b were probably produced by two hydrogen molecules removing and two oxygen molecules addition from the SMX compound. The amino group nitration in the benzene ring (TP283a as nitro-SMX (NO₂-SMX)) and methyl group oxidation to the carboxyl group in the isoxazole ring (TP283b) are other possible pathways. TP283a and TP283b can also be produced by SMX degradation using PMS activation by Fe(VI) [67] as well as direct oxidation

of Fe(VI) [68]. Breaking the bond between the benzene and sulfur ring in TP283a combination may result in the formation of TP123 and TP178, respectively [69]. The S-N bond cleavage between the sulfonyl and amine group in the sulfonamide group results in the formation of TP99 [3-amino-5-methylisoxazole (AMI)] as well as TP173 [sulfanilic acid (SNA)], which are widely reported as SMX TPs in the literature [34, 66, 69, 70]. Furthermore, the intermediates TP284a and TP253 could be cracked into TP99 [71–73]. TP156 (p-amino benzene sulfonic acid) was formed by S-N bond cleavage, where the formation of benzoquinone (TP108) was expected to be formed by the amine and sulfone groups hydroxylation in the SMX sulfanilic moiety [74]. TP502 (azosulfamethoxazole), a dimeric compound, was produced by coupling the N-centered radical derived from –NH₂ group via polymerization reactions [75, 76]. The formation of TP276 from the parent compound SMX has been attributed to its hydrolysis form and subsequently, TP292 belongs to the SMX degraded ions. These compounds have recently been reported in the photocatalytic degradation of SMX [77]. In another pathway, TP209 was identified. In the study of Li et al., 2020, the coupling of the N-(4-hydroxy-5-methylisoxazol-3-yl)-4-nitrobenzenesulfonamide (as m/z 300) to the oxazole ring through recombination of the N-centered radical derived from the –NH₂ group is the cause of TP209 formation [78]. But in this study, TP300 was not identified as a product. The S-C bond cleavage between sulfur and benzene ring resulted in TP94 (aniline). TP239 (N-(5-methylisozaxol-3-yl) benzenesulfonamide) indicates amine group cleavage in the isoxazole ring [70, 79]. Finally, further cleavage of benzoquinone ring and AMI can produce maleic acid, oxalic acid and pyruvic acid along with NH₄$^+$, NO₃$^-$, and SO₄$^{2-}$ [2, 80, 81]. In brief, (1) different bond-cleavage (2) rearrangement of the isoxazole ring (3) hydroxlation (4) carboxylation (5) nitration (6) polymerization (7) hydrolysis and (8) coupling reactions are the predominant degradation pathways in the SMX oxidation by Fe(VI).

Toxicity of SMX and its TPs

The ECOSAR is a simulation software that predicts acute (short-term) and chronic (long-term) toxicity of chemicals using computational methods [82–84]. In the present study, the toxicity of SMX and its degradation products were predicted by the ECOSAR program. The toxicity data according to the Globally Harmonized System of Classification and Labelling of Chemicals (GHS) was divided into four levels: not harmful (LC₅₀/EC₅₀/ChV > 100 mg/L), harmful (10 < LC₅₀/EC₅₀/ChV ≤ 100 mg/L), toxic (1 < LC₅₀/EC₅₀/ChV ≤ 10 mg/L) and very toxic (LC₅₀/EC₅₀/ChV ≤ 1 mg/L) [83]. As can be seen in Table 4, the parent compound (SMX) to be toxic or harmful towards all aquatic organisms, except for fish. In general, SMX
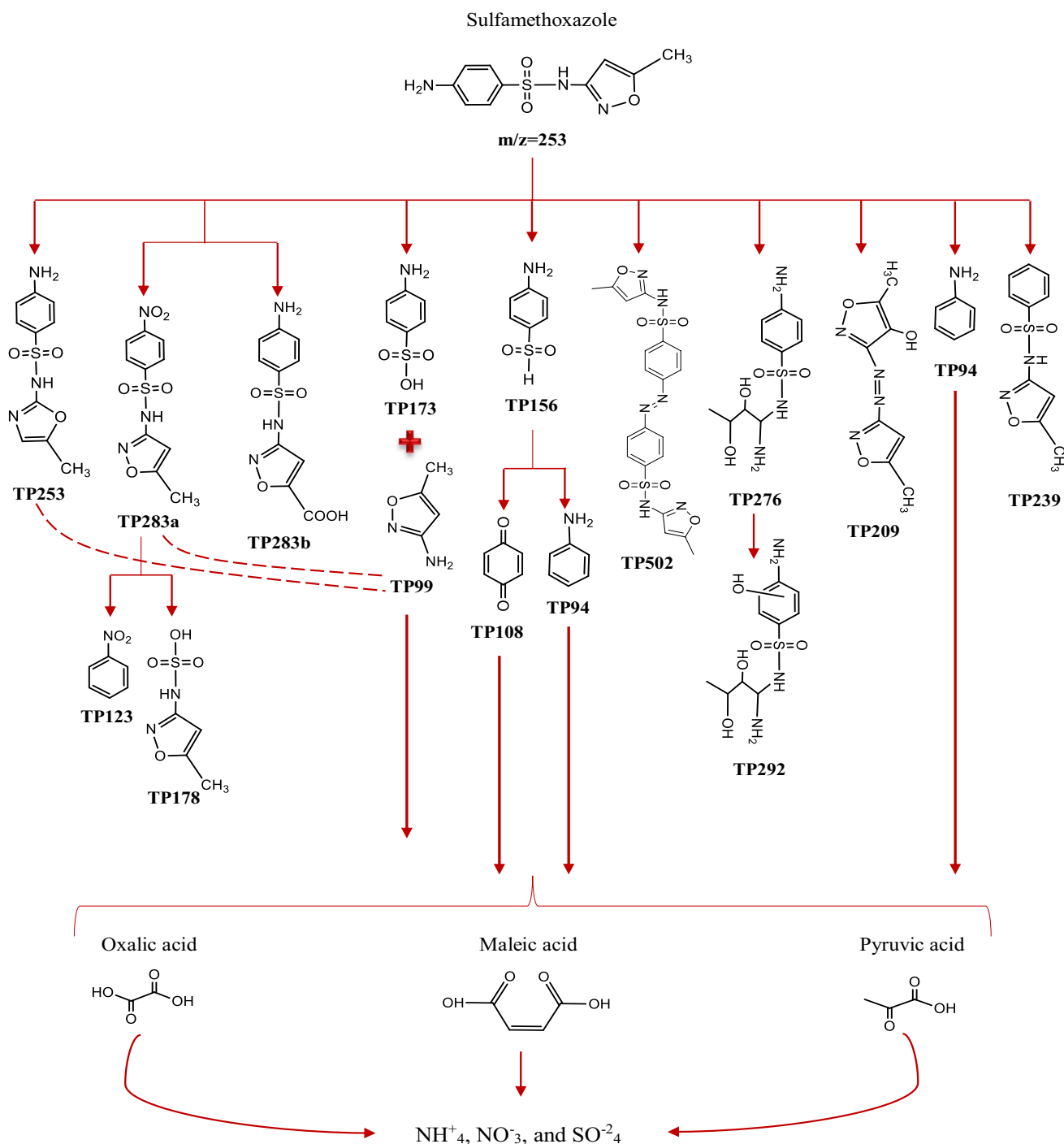
Fig. 2 Proposed reaction pathways of SMX oxidation by Fe(VI)

degradation products were toxic or harmful, except for five products (DP4, DP5, DP16, DP17, DP18) that were not harmful to the organisms. Also, the acute toxicity values of DP9 and DP14 are more than SMX for all organisms. Also, DP9 has the highest chronic toxicity for fish.

Conclusion

Potassium ferrate was used for SMX degradation under various experimental conditions. Under optimum

Table 3 Intermediate products of SMX degradation by potassium ferrate
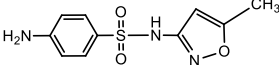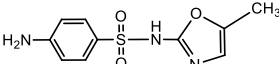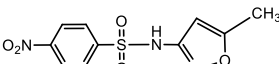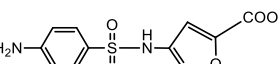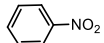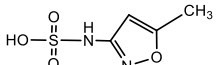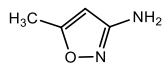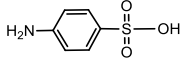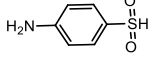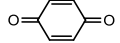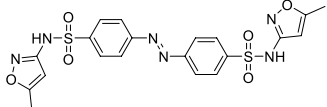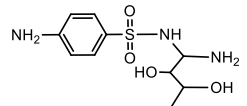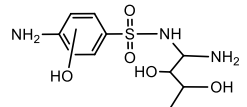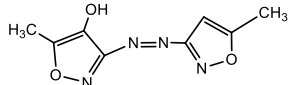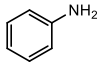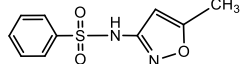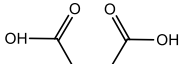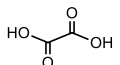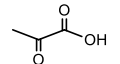
Compounds	M/Z	Chemical structures	Proposed formula
SMX	253		$C_{10}H_{11}N_3O_3S$
DP1	253		$C_{10}H_{11}N_3O_3S$
DP2	283a		$C_{10}H_9N_3O_5S$
DP3	283b		$C_{10}H_9N_3O_5S$
DP4	123		$C_6H_5NO_2$
DP5	178		$C_4H_6N_2O_4S$
DP6	99		$C_4H_6N_2O$
DP7	173		$C_6H_7NO_3S$
DP8	156		$C_6H_7NO_2S$
DP9	108		$C_6H_4O_2$
DP10	502		$C_{20}H_{18}N_6O_6S_2$
DP11	276		$C_{10}H_{17}N_3O_4S$
DP12	292		$C_{10}H_{18}N_3O_5S$
DP13	209		$C_8H_8N_4O_3$
DP14	94		C_6H_7N
DP15	239		$C_{10}H_{11}N_2O_3S$
DP16	116 (maleic acid)		$C_4H_4O_4$
DP17	90 (Oxalic acid)		$C_2H_2O_4$
DP18	88 (Pyruvic acid)		$C_3H_4O_3$

Table 4 Predicted toxicity of SMX and its transformation products by ECOSAR program

Compounds	Acute toxicity (mg L^{-1})			Chronic toxicity (mg L^{-1})		
	Fish (96 h-LC$_{50}$)	Daphnia (48 h-LC$_{50}$)	Green Algae (96 h-EC$_{50}$)	Fish (ChV)	Daphnia (ChV)	Green Algae (ChV)
SMX	266.77	6.43	21.82	5	0.07	11.14
DP1	266.77	6.43	21.82	5	0.07	11.14
DP2	16,855.71	25,742.14	689.84	59.48	1422.88	117.99
DP3	11,779.54	123.43	490.32	321.63	1.2	365.57
DP4	14,276.3	6501.37	1944.88	1075.72	343.09	311.6
DP5	8,651,950	3,007,865.25	294,745	474,137.25	74,888.76	25,887.29
DP6	270.05	3.63	13.77	6.59	0.04	9.16
DP7	86,326.91	200.34	1059.05	4650.41	1.67	1565.55
DP8	1328.68	9.05	39.02	44.05	0.08	35.37
DP9	0.09	0.74	0.05	0.01	4.87	0.01
DP10	26.53	22.43	4.52	0.52	5.22	4.34
DP11	91,793.12	67.22	442.19	8316.86	0.5	1103.6
DP12	199,901.48	94.46	675.19	22,066.26	0.67	2055.96
DP13	105.81	31.49	9.03	9.63	2.98	15.72
DP14	40.29	1.67	5.1	0.59	0.02	2.04
DP15	195.26	207.96	19.06	1.96	27.62	9.34
DP16	53,316.05	25,294.8	8964.33	4216.2	1496.17	1573.47
DP17	167,790.03	67,473.03	12,070.37	10,917.65	2519.06	1466.06
DP18	59,171.71	24,903.57	5378.23	4062.66	1055.41	722.97

experimental conditions and extended contact time, Fe(VI) was found to be a promising oxidant for SMX removal from secondary treated effluents. TOC analysis indicated that SMX mineralization in this process was not very successful, suggesting some TPs formation. Also, the kinetic study under two pH conditions indicated that the degradation rate under the acidic pH was 7.6 times higher than the neutral condition. SMX removal in the presence of phosphate and EDTA was dramatically declined during the process. While Fe(III) could enhance SMX degradation in earlier reaction time, degradation efficiency declined dramatically by increasing reaction time and iron dosage. Transformation, bond cleavage (mainly sulfonamide bond), as well as transformation after cleavage were the most degradation mechanisms proposed for SMX degradation by Fe(VI). Toxicity assessment showed that harmful Fe(VI) oxidation byproducts could be produced.

Code availability Not applicable for this study.

Authors contribution All authors contributed to the study conception and design. Material preparation, data collection and analysis were performed by [Behjat Jebalbarezi], [Reza Dehghanzadeh], [Samira Sheikhi], [Najmeh Shahmahdi], [Hassan Aslani] and [Ammar Maryamabadi]. The first draft of the manuscript was written by [Behjat Jebalbarezi] and all authors commented on previous versions of the manuscript. All authors read and approved the final manuscript.

Declarations

Conflict of interest The authors declare that they have no conflict of interest.

Ethics approval Not applicable for this study.

Consent to participate No human and/or animals participated in this study.

Consent for publication Not applicable for this study.

References

1. Das I, Das S, Chakraborty I, Ghangrekar M. Bio-refractory pollutant removal using microbial electrochemical technologies: a short review. J Indian Chem Soc. 2019;96:493–7.

2. Dirany A, Sirés I, Oturan N, Oturan MA. Electrochemical abatement of the antibiotic sulfamethoxazole from water. Chemosphere. 2010;81:594–602.

3. Gagnon C, Lajeunesse A, Cejka P, Gagne F, Hausler R. Degradation of selected acidic and neutral pharmaceutical products in a primary-treated wastewater by disinfection processes. Ozone Sci Eng. 2008;30:387–92.

4. Lewis K. Platforms for antibiotic discovery. Nat Rev Drug Discov. 2013;12:371.

5. Van Boeckel TP, Brower C, Gilbert M, Grenfell BT, Levin SA, Robinson TP, et al. Global trends in antimicrobial use in food animals. Proc Natl Acad Sci. 2015;112:5649–54.

6. Gothwal R, Shashidhar T. Antibiotic pollution in the environment: a review. Clean–Soil, Air, Water. 2015;43:479–89.

7. Carvalho IT, Santos L. Antibiotics in the aquatic environments: a review of the European scenario. Environ Int. 2016;94:736–57.

8. Elmolla ES, Chaudhuri M. Comparison of different advanced oxidation processes for treatment of antibiotic aqueous solution. Desalination. 2010;256:43–7.

9. Kim HY, Kim T-H, Cha SM, Yu S. Degradation of sulfamethoxazole by ionizing radiation: identification and characterization of radiolytic products. Chem Eng J. 2017;313:556–66.

10. Daouk S, Chevre N, Vernaz N, Bonnabry P, Dayer P, Daali Y, et al. Prioritization methodology for the monitoring of active pharmaceutical ingredients in hospital effluents. J Environ Manag. 2015;160:324–32.

11. Sharma VK, Johnson N, Cizmas L, McDonald TJ, Kim H. A review of the influence of treatment strategies on antibiotic resistant bacteria and antibiotic resistance genes. Chemosphere. 2016;150:702–14.

12. Luo Y, Guo W, Ngo HH, Nghiem LD, Hai FI, Zhang J, et al. A review on the occurrence of micropollutants in the aquatic environment and their fate and removal during wastewater treatment. Sci Total Environ. 2014;473:619–41.

13. Asif MB, Ansari AJ, Chen S-S, Nghiem LD, Price WE, Hai FI. Understanding the mechanisms of trace organic contaminant removal by high retention membrane bioreactors: a critical review. Environ Sci Pollut Res. 2019;26:34085–100.

14. García-Muñoz P, Pliego G, Zazo JA, Munoz M, de Pedro ZM, Bahamonde A, et al. Treatment of hospital wastewater through the CWPO-Photoassisted process catalyzed by ilmenite. 2017;5:4337-43.

15. Gad-Allah TA, Ali ME, Badawy MI. Photocatalytic oxidation of ciprofloxacin under simulated sunlight. J Hazard Mater. 2011;186:751–5.

16. Lin AY-C, Lin C-F, Chiou J-M, Hong PA. O3 and O3/H2O2 treatment of sulfonamide and macrolide antibiotics in wastewater. J Hazard Mater. 2009;171:452–8.

17. Garoma T, Umamaheshwar SK, Mumper A. Removal of sulfadiazine, sulfamethizole, sulfamethoxazole, and sulfathiazole from aqueous solution by ozonation. Chemosphere. 2010;79:814–20.

18. Shen Z, Fan L, Yang S, Yao Y, Chen H, Wang W. Fe-based carbonitride as Fenton-like catalyst for the elimination of organic contaminants. Environ. Res. 2020;110486.

19. McQuarters AB, Wolf MW, Hunt AP, Lehnert N. 1958-2014: after 56 years of research, cytochrome p450 reactivity is finally explained. Angewandte Chemie (International ed in English). 2014;53:4750–2.

20. Bandala ER, Miranda J, Beltran M, Vaca M, Lopez R, Torres LG. Wastewater disinfection and organic matter removal using ferrate (VI) oxidation. J Water Health. 2009;7:507–13.

21. Luo Z, Li X, Zhai J. Kinetic investigations of quinoline oxidation by ferrate(VI). Environ Technol. 2016;37:1249–56.

22. Delaude L, Laszlo P. A novel oxidizing reagent based on potassium ferrate(VI)(1). J Org Chem. 1996;61:6360–70.

23. Ma J, Liu W. Effectiveness of ferrate (VI) preoxidation in enhancing the coagulation of surface waters. Water Res. 2002;36:4959–62.

24. Graham N, Jiang CC, Li XZ, Jiang JQ, Ma J. The influence of pH on the degradation of phenol and chlorophenols by potassium ferrate. Chemosphere. 2004;56:949–56.

25. Al-Muzaini S. Industrial wastewater management in Kuwait. Desalination. 1998;115:57–62.

26. Sharma VK, Luther GW 3rd, Millero FJ. Mechanisms of oxidation of organosulfur compounds by ferrate(VI). Chemosphere. 2011;82:1083–9.

27. Jain A, Sharma VK, Mbuya OS. Removal of arsenite by Fe(VI), Fe(VI)/Fe(III), and Fe(VI)/Al(III) salts: effect of pH and anions. J Hazard Mater. 2009;169:339–44.

28. Noorhasan N, Patel B, Sharma VK. Ferrate(VI) oxidation of glycine and glycylglycine: kinetics and products. Water Res. 2010;44:927–35.

29. Zheng L, Deng Y. Settleability and characteristics of ferrate(VI)-induced particles in advanced wastewater treatment. Water Res. 2016;93:172–8.

30. Aslani H, Nabizadeh R, Nasseri S, Mesdaghinia A, Alimohammadi M, Mahvi AH, et al. Application of response surface methodology for modeling and optimization of trichloroacetic acid and turbidity removal using potassium ferrate (VI). Desalination Water Treat. 2016;57:25317–28.

31. Deng J, Wu H, Wang S, Liu Y, Wang H. Removal of sulfapyridine by ferrate (VI): efficiency, influencing factors and oxidation pathway. Environ Technol. 2019;40:1585–91.

32. Feng M, Cizmas L, Wang Z, Sharma VK. Activation of ferrate (VI) by ammonia in oxidation of flumequine: kinetics, transformation products, and antibacterial activity assessment. Chem Eng J. 2017;323:584–91.

33. Jiang J, Zhou Z. Removal of pharmaceutical residues by ferrate (VI). PLoS One. 2013;8:e55729.

34. Kim C, Panditi VR, Gardinali PR, Varma RS, Kim H, Sharma VK. Ferrate promoted oxidative cleavage of sulfonamides: kinetics and product formation under acidic conditions. Chem Eng J. 2015;279:307–16.

35. Sharma VK, Mishra SK, Ray AK. Kinetic assessment of the potassium ferrate (VI) oxidation of antibacterial drug sulfamethoxazole. Chemosphere. 2006;62:128–34.

36. Zhang K, Luo Z, Zhang T, Gao N, Ma Y. Degradation effect of sulfa antibiotics by potassium ferrate combined with ultrasound (Fe(VI)-US). Biomed Res Int. 2015;2015:12.

37. Greenberg AE, Clesceri LS, Eaton AD. Standard methods for the examination of water and wastewater: J. Am. Public Health Assoc. 1992.

38. Bhattacharyya KG, Gupta SS. Kaolinite, montmorillonite, and their modified derivatives as adsorbents for removal of cu (II) from aqueous solution. Sep Purif Technol. 2006;50:388–97.

39. Rush JD, Zhao Z, Bielski BH. Reaction of ferrate (VI)/ferrate (V) with hydrogen peroxide and superoxide anion-a stopped-flow and premix pulse radiolysis study. Free Radic Res. 1996;24:187–98.

40. Chen J, Xu X, Zeng X, Feng M, Qu R, Wang Z, et al. Ferrate (VI) oxidation of polychlorinated diphenyl sulfides: kinetics, degradation, and oxidized products. Water Res. 2018;143:1–9.

41. Jiang JQ. Research progress in the use of ferrate(VI) for the environmental remediation. J Hazard Mater. 2007;146:617–23.

42. Li C, Li X, Graham N, Gao N. The aqueous degradation of bisphenol a and steroid estrogens by ferrate. Water Res. 2008;42:109–20.

43. Feng M, Wang X, Chen J, Qu R, Sui Y, Cizmas L, et al. Degradation of fluoroquinolone antibiotics by ferrate (VI): effects of water constituents and oxidized products. Water Res. 2016;103:48–57.

44. Fan X, Hao H, Shen X, Chen F, Zhang J. Removal and degradation pathway study of sulfasalazine with Fenton-like reaction. J Hazard Mater. 2011;190:493–500.

45. Maiakootian M, Asadi M. Efficiency of fenton oxidation process in removal of phenol in aqueous solutions. 2011.

46. Pignatello JJ, Oliveros E, MacKay A. Advanced oxidation processes for organic contaminant destruction based on the Fenton reaction and related chemistry. Crit Rev Environ Sci Technol. 2006;36:1–84.

47. Hu P, Yang B, Dong C, Chen L, Cao X, Zhao J, et al. Assessment of EDTA heap leaching of an agricultural soil highly contaminated with heavy metals. Chemosphere. 2014;117:532–7.

48. Jiang J, Pang SY, Ma J. Role of ligands in permanganate oxidation of organics. Environ Sci Technol. 2010;44:4270–5.

49. Andrade MD, Prasher SO, Hendershot WH. Optimizing the molarity of a EDTA washing solution for saturated-soil remediation of trace metal contaminated soils. Environ Pollut (Barking, Essex : 1987). 2007;147:781-90.

50. Fan J, Lin B-H, Chang C-W, Zhang Y, Lin T-F. Evaluation of potassium ferrate as an alternative disinfectant on cyanobacteria inactivation and associated toxin fate in various waters. Water Res. 2018;129:199–207.

51. Kolář M, Novák P, Šišková KM, Machala L, Malina O, Tuček J, et al. Impact of inorganic buffering ions on the stability of Fe (VI) in aqueous solution: role of the carbonate ion. Phys Chem. 2016;18:4415–22.

52. Zhao J, Liu Y, Wang Q, Fu Y, Lu X, Bai X. The self-catalysis of ferrate (VI) by its reactive byproducts or reductive substances for the degradation of diclofenac: kinetics, mechanism and transformation products. Sep Purif Technol. 2018;192:412–8.

53. Rush J, Bielski BH. Kinetics of ferrate (V) decay in aqueous solution. A pulse-radiolysis study Inorg Chem. 1989;28:3947–51.

54. Rizvi MA. Complexation modulated redox behavior of transition metal systems. Russ J Gen Chem. 2015;85:959–73.

55. Huang Z-S, Wang L, Liu Y-L, Jiang J, Xue M, Xu C-B, et al. Impact of phosphate on ferrate oxidation of organic compounds: an underestimated oxidant. Environ Sci Technol. 2018;52:13897–907.

56. Sharma VK, Burnett CR, Millero FJ. Dissociation constants of the monoprotic ferrate (VI) ion in NaCl media. Phys Chem Chem Phys. 2001;3:2059–62.

57. Boreen AL, Arnold WA, McNeill K. Photochemical fate of sulfa drugs in the aquatic environment: sulfa drugs containing five-membered heterocyclic groups. Environ Sci Technol. 2004;38:3933–40.

58. Sharma VK, Burnett CR, O'Connor DB, Cabelli D. Iron (VI) and iron (V) oxidation of thiocyanate. Environ Sci Technol. 2002;36:4182–6.

59. Sharma VK, Rendon RA, Millero FJ, Vazquez FG. Oxidation of thioacetamide by ferrate (VI). Mar Chem. 2000;70:235–42.

60. Sharma VK, Rivera W, Joshi VN, Millero FJ, O'Connor D. Ferrate (VI) oxidation of thiourea. Environ Sci Technol. 1999;33:2645–50.

61. Han H, Li J, Ge Q, Wang Y, Chen Y, Wang B. Green ferrate (VI) for multiple treatments of fracturing wastewater: Demulsification, visbreaking, and chemical oxygen demand removal. Int J Mol Sci. 2019;20:1857.

62. Martins RC, Dantas RF, Sans C, Esplugas S, Quinta-Ferreira RM. Ozone/H2O2 performance on the degradation of sulfamethoxazole. Ozone Sci Eng. 2015;37:509–17.

63. Dirany A, Sirés I, Oturan N, Özcan A, Oturan MA. Electrochemical treatment of the antibiotic sulfachloropyridazine: kinetics, reaction pathways, and toxicity evolution. Environ Sci Technol. 2012;46:4074–82.

64. Shahmahdi N, Dehghanzadeh R, Aslani H, Shokouhi SB. Performance evaluation of waste iron shavings (Fe0) for catalytic ozonation in removal of sulfamethoxazole from municipal wastewater treatment plant effluent in a batch mode pilot plant. Chem Eng J. 2019;123093.

65. Abellan M, Gebhardt W, Schröder HF. Detection and identification of degradation products of sulfamethoxazole by means of LC/MS and− MSn after ozone treatment. Water Sci Technol. 2008;58:1803–12.

66. Gong H, Chu W. Determination and toxicity evaluation of the generated products in sulfamethoxazole degradation by UV/CoFe2O4/TiO2. J Hazard Mater. 2016;314:197–203.

67. Gong H, Chu W, Xu K, Xia X, Gong H, Tan Y, et al. Efficient degradation, mineralization and toxicity reduction of sulfamethoxazole under photo-activation of peroxymonosulfate by ferrate (VI). Chem. Eng. J. 2020;124084.

68. Zhou Z, Jiang J-Q. Treatment of selected pharmaceuticals by ferrate (VI): performance, kinetic studies and identification of oxidation products. J Pharm Biomed Anal. 2015;106:37–45.

69. Zhuan R, Wang J. Enhanced mineralization of sulfamethoxazole by gamma radiation in the presence of Fe 3 O 4 as Fenton-like catalyst. Environ Sci Pollut Res. 2019;26:27712–25.

70. Su T, Deng H, Benskin JP, Radke M. Biodegradation of sulfamethoxazole photo-transformation products in a water/sediment test. Chemosphere. 2016;148:518–25.

71. Trovó AG, Nogueira RF, Agüera A, Sirtori C, Fernández-Alba AR. Photodegradation of sulfamethoxazole in various aqueous media: persistence, toxicity and photoproducts assessment. Chemosphere. 2009;77:1292–8.

72. He Y, Zhang J, Zhou H, Yao G, Lai B. Synergistic multiple active species for the degradation of sulfamethoxazole by peroxymonosulfate in the presence of CuO@ FeOx@ Fe0. Chem Eng J. 2020;380:122568.

73. Wang H, Wang S, Jiang J-Q, Shu J. Removal of sulfadiazine by ferrate (VI) oxidation and montmorillonite adsorption—synergistic effect and degradation pathways. J Environ Chem Eng. 2019;7:103225.

74. Yin R, Guo W, Du J, Zhou X, Zheng H, Wu Q, et al. Heteroatoms doped graphene for catalytic ozonation of sulfamethoxazole by metal-free catalysis: performances and mechanisms. Chem Eng J. 2017;317:632–9.

75. Gao S, Zhao Z, Xu Y, Tian J, Qi H, Lin W, et al. Oxidation of sulfamethoxazole (SMX) by chlorine, ozone and permanganate—a comparative study. J Hazard Mater. 2014;274:258–69.

76. Milh H, Schoenaers B, Stesmans A, Cabooter D, Dewil R. Degradation of sulfamethoxazole by heat-activated persulfate oxidation: elucidation of the degradation mechanism and influence of process parameters. Chem Eng J. 2020;379:122234.

77. Jahdi M, Mishra SB, Nxumalo EN, Mhlanga SD, Mishra AK. Smart pathways for the photocatalytic degradation of sulfamethoxazole drug using F-Pd co-doped TiO2 nanocomposites. Appl Catal B. 2020;267:118716.

78. Li Y, Li J, Pan Y, Xiong Z, Yao G, Xie R, et al. Peroxymonosulfate activation on FeCo2S4 modified g-C3N4 (FeCo2S4-CN): mechanism of singlet oxygen evolution for nonradical efficient degradation of sulfamethoxazole. Chem Eng J. 2020;384:123361.

79. Poirier-Larabie S, Segura P, Gagnon C. Degradation of the pharmaceuticals diclofenac and sulfamethoxazole and their transformation products under controlled environmental conditions. Sci Total Environ. 2016;557:257–67.

80. Wang A, Li Y-Y, Estrada AL. Mineralization of antibiotic sulfamethoxazole by photoelectro-Fenton treatment using activated carbon fiber cathode and under UVA irradiation. Appl. Catal. B. 2011;102:378–86.

81. García-Munoz P, Pliego G, Zazo J, Bahamonde A, Casas J. Sulfonamides photoassisted oxidation treatments catalyzed by ilmenite. Chemosphere. 2017;180:523–30.

82. Xu X, Chen J, Qu R, Wang Z. Oxidation of tris (2-chloroethyl) phosphate in aqueous solution by UV-activated peroxymonosulfate: kinetics, water matrix effects, degradation products and reaction pathways. Chemosphere. 2017;185:833–43.

83. Tay KS, Madehi N. Ozonation of ofloxacin in water: by-products, degradation pathway and ecotoxicity assessment. Sci Total Environ. 2015;520:23–31.

84. Quaresma AV, Sousa BA, Silva KT, Silva SQ, Werle AA, Afonso RJ. Oxidative treatments for atenolol removal in water: elucidation by mass spectrometry and toxicity evaluation of degradation products. Rapid Commun Mass Spectrom. 2019;33:303–13.

85. Wu K, Wang H, Zhou C, AminaY Y. Si, efficient oxidative removal of sulfonamide antibiotics from the wastewater by potassium ferrate. J Adv Oxid Technol. 2018;21:97–108.

86. Zhou J-H, Chen K-B, Hong Q-K, Zeng F-C, Wang H-Y. Degradation of chloramphenicol by potassium ferrate (VI) oxidation: kinetics and products. Environ Sci Pollut Res. 2017;24:10166–71.

87. Zhao J, Liu Y, Wang Q, Fu Y, LuX X. Bai, the self-catalysis of ferrate (VI) by its reactive byproducts or reductive substances for the degradation of diclofenac: kinetics, mechanism and transformation products. Sep Purif Technol. 2018;192:412–8.